International Journal of Integrated Engineering: Special Issue 2018: Innovations in Civil Engineering, Vol. 10 No. 9 (2018) p. 108-112

DOI: https://doi.org/10.30880/ijie.2018.10.09.020

Physical characterization and electrical conductivity of $Li_{1.2}Ti_{1.8}Al_{0.2}(PO_4)_3$ and $Li_{1.2}Ta_{0.9}Al_{1.1}(PO_4)_3$ NASICON material

Mohammed Isah Kimpa*[1,2], Mohd Zul Hilmi Bin Mayzan[2], Fahmiruddin Esa[2], Jibrin Alhaji Yabagi[2,3], Muhammad Muhammad Nmaya[2,3] and Mohd Arif Bin Agam[2]

[1] Department of Physics, School of Physical Science, Federal University of Technology Minna, P.M.B. 64, Minna, Niger State, Nigeria.
[2] Materials Physics Laboratory, Faculty of Applied Science and Technology, Bandar University, 84600, Pagoh, Universiti Tun Hussein Onn Malaysia, 84500 Pagoh, Johor, Malaysia.
[3] Department of Physics, Faculty of Natural Sciences, Ibrahim Badamasi Babangida University Lapai, P.M.B. 10, Lapai, Niger State, Nigeria.

Received 17 March 2018; accepted 27 December 2018, available online 31 December 2018

Abstract: Sodium superionic conducting materials (NASICON) are promising solid electrolytes for Li-ion batteries and suitable to be used in the area that requires high energy density as well as rechargeable power sources. Fabrication of all-solid-state Li battery with non-flammable ceramics electrolyte has been strongly required to solve safety issues of present Li batteries. In this study, lithium titanium aluminium phosphate $Li_{1+x}Ti_{2-x}Al_x(PO_4)_3$, LTAP ($x$ = 0.2) and lithium tantalum aluminium phosphate $Li_{1+2x}Ta_{1-x}Al_{x+1}(PO_4)_3$, LTaAP ($x$ = 0.1) were prepared via conventional solid state reaction techniques at various sintering temperature ranging from 700 to 1000 °C. LTAP and LTaAP compositions attain their optimum sintering temperature at 800 °C. Physical properties of LTAP and LTaAP show the bulk density of 2.83 and 3.63 g/cm^3 which resulted into high densification of the material. The XRD analysis revealed NASICON crystalline phase dominated by $LiTi_2(PO_4)_3$ and minor impurity phases for LTaAP composition. Bulk conductivity values for LTAP and LTaAP were found to be 1.06 x 10^{-4} and 9.854 x 10^{-6} S/cm at room temperature. LTAP had better conductivity behavior compare to LTaAP composition which could be due to differences in their ionic radius (titanium, 0.605 nm tantalum, 0.64 nm and the aluminium, 0.53 nm) in sizes, though the conductivity obtained for both compositions has the capacity to serve as solid electrolyte material could be used in lithium ion rechargeable battery.

Keywords: Li battery, solid electrolyte, solid-state reaction route, conductivity

1. Introduction

The advent of solid state batteries must be understood in the context of the challenges faced by modern storage systems, expecially lithium ion battery [1]. Much attention has been paid to rechargeable lithium batteries as a future energy storage due to its higher energy density and longer charge retention [2].

Lithium-based solid electrolyte is one of the best candidates for the application in batteries due to its high potential and low weight for high-energy density storage in batteries [3]. The lithium transition metal phosphates have found application in the field of electrochemical energy storage, especially those with Nasicon structure, because of their good electrochemical performances and capability to answer safety concerns surrounding oxide chemistry [4].

Despite the attractive features of NASICON LATP, it is not clear whether the high conductivity of $Li_{1+x}Ti_{2-x}Al_x(PO_4)_3$ composition is intrinsic to the structure or the formation of secondary phases that favors sintering and eliminate grain-boundary resistance is the cause of high conductivity [5], [6]. Towards this end, lithium-ion conduction of mixed-metal NASICON-phases of the formula, $LiM^{v}M^{iii}(PO_4)_3$, where M^V = Nb, Ta; M^{iii} = Al, Cr, Fe were examined to obtained a NASICON phase possessing intrinsic conducting properties similar to $LiTi_2(PO_4)_3$ but without Ti^{iv} [6].

The planetary mono mill is a technique that uses a high energy ball mill for synthesizing solid electrolyte materials to achieve phase homogeneity of the final product. However, the use of this milling machine is a well-known technique and has attracted the interest of

many researchers for preparing nano-sized materials [7]–[9].

In this work, lithium titanium aluminium phosphate (LTAP) and lithium tantalum aluminium phosphate (LTaAP) NASICON ceramics were prepared using conventional solid state reaction method, which requires mono milling procedure and sintering processes. The main aim is to investigate the ionic conductivity and structural phase purity of the prepared sample using XRD, FESEM and impedance spectroscopy based on the optimum sintering data obtained from density measurement.

2. Methodology

2.1 Starting material synthesis

Lithium titanium aluminium phosphate, LTAP and lithium tantalum aluminium phosphate, LTaAP compositions were synthesized using different starting material grade. LTAP and LTaAP was prepared using lithium carbonate (Li_2CO_3), titanium dioxide (TiO_2), tantalum oxide (Ta_2O_5), aluminium dioxide (Al_2O_3) and ammonium dihydrogen phosphate ($NH_4H_2PO_4$). All the raw materials were certified as reagent grade and originated from R&M Marketing, Essex, U.K and Alfa Aesar companies. In each case, the precursors have been weighed accordingly to their ratios and grounded for 1 h using agate mortar and pestle; 10 ml of acetone was added to the mixture to achieve homogeneity. LTAP mixture was initially calcined at 450 °C for 1.5 h and further calcined at 900 °C for 2 h in alumina crucible, and LTaAP composition was calcined twice at 600 °C for 2h each. The initial heating was intended to decompose Li_2CO_3 and $NH_4H_2PO_4$ into ammonia, carbon dioxide, and water. The calcined samples were re-grounded using planetary mono milling with zirconia jar and balls as grinding media for 5 h at 450 rpm. The samples were pressed into a pellet of 1.3 cm diameter and 2-3 mm thickness at a pressure of 5 tons. The pellet samples were sintered from 800 to 1000 °C for 8 and 12 h for LTAP and LTaAP respectively. After polishing down to 1 µm finish, the smooth surface of sintered pellets was dried at 100 °C for 2 h and stored at room temperature for further examination. The bulk density was measured using Archimedes principle (Mettler Toledo density balance XS64) to investigate the effect of sintering on each composition. Distilled water was used as the immersion liquid medium at room temperature during the measurement. LTAP and LTaAP samples will be designated as LTAP-0.2 and LTaAP-0.1 in the figures presented in this study.

2.2 Characterization techniques

The structural identification of the LTAP-0.2 and LTaAP-0.1 samples were characterized using X-ray diffraction (XRD PANalytical) in 2θ range of 10 – 40° using Cu-kα radiation). Field emission scanning electron microscope (FESEM-JEOL, JSM-7600F) was used to investigate the surface morphology of the LTAP-0.2 while scanning electron microscope (SEM) equipped with an EDS (Hitachi SEM) was used to investigate surface morphology of LTaAP-0.1 sample. Pure gold was used to coat the sample prior to the image scanning. The electrical impedance response was recorded by an impedance analyser (Agilent impedance spectroscopy) in a frequency range between 40 Hz and 2 MHz at room temperature.

3 Results and Discussion

3.1 Bulk density measurement

Fig. 1 shows the bulk density of LTAP and LTaAP compositions. LTAP is sintered from 800 to 1000 °C while LTaAP was sintered from 700 to 1000 °C. The bulk density of 2.91 g/cm^3 at 800 °C sintering temperature was observed for LTAP sample. Further increase in temperature, suddenly decreases the density to 2.65 g/cm^3 at 850 °C and the density further increase to 2.83 g/cm^3. Bulk density decreases with increase in temperature from 900 to 950 °C with slight increase of density at 1000 °C sintering temperature. The decrease in bulk density which occurs at 950 and 1000 °C for LTAP-0.2 could be as a result of voids that probably do occur between the individual grains which lead to low density of ceramic materials. High densification of crystal grains occurs at 800 °C sintering temperature with bulk density of 2.91 g/cm^3. At this temperature, the sample is denser with minimum or no voids along the grain boundaries and resulted in higher densification.

LTaAP increase from 700 °C sintering temperature to 800 °C and suddenly decrease with increase in temperature up to 1000 °C. LTaAP has high bulk density of 3.52 g/cm^3 at 800 °C sintering temperature. This material attains it maximum crystallization at 800 °C sintering condition. LTAP and LTaAP materials reach their maximum crystallinity at 800 °C.

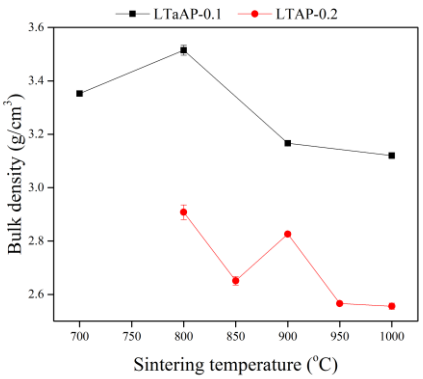

Fig.1 Bulk Density curve at different sintering temperature for LTAP-0.2 and LTaAP-0.1 composition.

3.2 X-ray diffraction of LTAP and LTaAP compositions

The typical XRD patterns for the sintered specimens (LTAP and LTaAP) are shown in Fig. 2. All the peaks were indexed based on the rhombohedral NASICON R-3c structure except for LTaAP samples with minor peaks marked by circle at 2θ = 27.6 and 32.1 °. The minor

phase in LTaAP (indicated by red circle) in Ta substituted specimens have been identified as $AlPO_4$. LTAP-0.2 shows a pure material without any impurity which could be the reason for having better conductivity compared to LTaAP sample or due to differences in ionic radius of the substituted elements Ta^{5+} (0.64 nm) and Ti^{4+} (0.605 nm) with Al^{3+} (0.53 nm) content. It is observed from the graph that LTaAP samples grow crystalline peaks longer with high intensity at (104) miller indices (higher peaks) compared to LTAP sample, though, higher intensities for $LiTi_2(PO4)_3$ compositions occurs at (113) orientation [10], [11]. The differences observed in terms of peak elongation for the two compositions could somehow be due to variation in the ionic radius as stated earlier above, previosly, some researchers on LTAP compositions observed peak shift towards higher or lower 2θ [12], [13]. The x-ray diffraction study clearly shows that the substitution of Ta^{5+} with Al^{3+} as well as Ti^{4+} with Al^{3+} can leads to changes in the structural parameters, which is caused by a quantitative change of the stoichiometric amount of *x*-variable in the compounds [14],[15]. This could be one of the reasons for the differences in the phases of LTAP and LTaAP compositions.

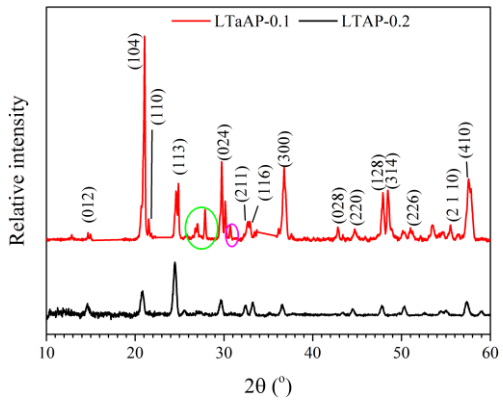

Fig.2 XRD pattern of LTAP-0.2 and LTaAP-0.1 sintered at different temperature.

3.3 Microstructural analysis of LTAP and LTaAP compositions

Fig.3 (a) shows the microstructure of the sintered pellet of LTAP, while Fig. 3(b) and (c) depicts the surface morphology of LTaAP-0.1 at different magnification of 3K and 7.5K respectively. The difference in the morphology of LTAP and LTaAP observed from the micrograph shows primarily the NASICON rectangular cubic structure with crystalline neck growth among the particles for LTAP. LTaAP sample has no discernible crystalline grains except at the region with pores (indicated by red rectangular cubic). This area of pores observed for LTaAP-0.1 shows crystalline grains and NASICON cubic structure when viewed at higher magnification of 7.5K.

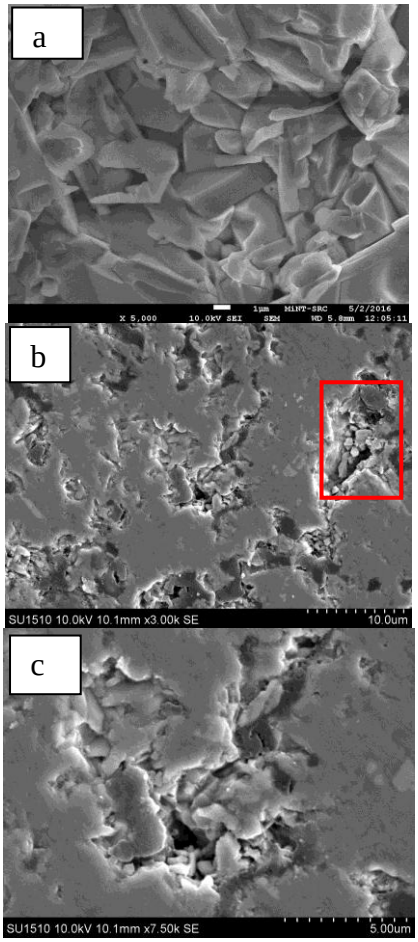

Fig. 3 Microstructural surface for (a) FESEM image of LTAP-0.2 sintered at 900 °C, (b) SEM image of LTaAP-0.1 at 3 k magnification and (c) LTaAP-0.1 at 7.5 k magnification sintered at 800 °C.

3.4 Electrical properties of LTAP and LTaAP compositions

The impedance spectra were fitted based on the electrical equivalent circuit show in Fig. 4 (a and b) for LTAP and LTaAP compositions respectively. Resistance of current electrode (*R1*) and two semi-circles were observed in the impedance plots for LTAP sample (Fig. 4-a). LTaAP comprises of 3 consecutive arrays: Z1*, Z2* and Z3* which are corresponding to the contribution of bulk, grain boundaries and electrode to the total impedance which was revealed by the equivalent circuits' analysis (Fig. 4-b). Each element of the impedance for bulk and grain boundary can be represented as a combination of parallel resistor (Rb and Rgb) connected with a constant phase element (CPE1 and CPE2) and the 3rd circuit is the electrode electrolyte interface (CPE3). The depressed semicircles observed from the fitted equivalent circuit imply that the grains (bulk) and grain boundary resistance overlap on each other and resulted into the constant phase element for both semicircles. In aluminium doped samples particularly, the overlap of

both semicircles does arise because grain and grain boundary contributions to conductivity are almost very close in frequency. This could be ascribed as due to low electrical homogeneity of the samples. The conflict in the interpretations of semicircles which is not identifiable from the Nyquist plot was clarified when fitted with the equivalent circuit used in this study (Fig 4-a&b). Data generated from the fitted equivalent circuit was used to obtain the bulk, grain boundary conductivity with the relation in equation 1:

$$\sigma = \frac{t}{RA} \tag{1}$$

where *"σ"* is the dc conductivity, *"t"* is the sample thickness, *"R"* is the resistance value along *x*-axis of the impedance plot and *"A"* is the area of the sample. Fig. 5 shows the impedance spectroscopy measurement for LTAP and LTaAP compositions. The resultant bulk conductivities for LTAP and LTaAP were 1.06 x 10^{-4} and 9.8 x 10^{-6} S/cm respectively measured at room temperature. LTAP having higher electrical conductivity compare to LTaAP from the impedance analysis is an indication that LTAP composition in this study have better compact of atoms within their lattice frame work in comparison to LTaAP sample. The impedance spectra for LTAP have lower radius with low resistance along the real axis of Nyquist plot compare to LTaAP samples. This could also be one of the reasons for LTaAP low conductivity in this study. The decrease in semicircle for NASICON materials indicate low grain boundary of that materials, since the grain boundary contribution to conductivity determine the ionic diffusivity and fast movement of Li ion mobility from M1 and M2 cavity of NASICON framework. This result shows higher conductivity compare to result obtained for the same composition and similar synthetic route for LTAP compound [9, 15] at room temperature as 1.44 x 10^{-5} S/cm and ~ 10^{-7}.

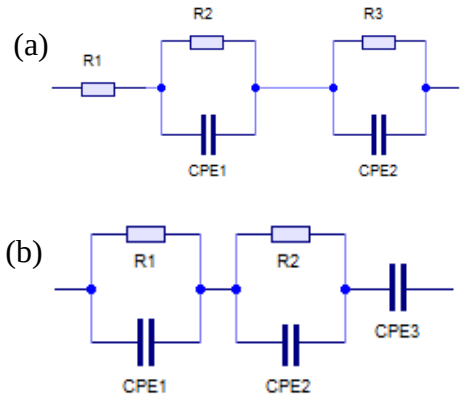

Fig. 4 Equivalent circuit for (a) LTAP-0.2 and (b) LTaAP-0.1 compositions

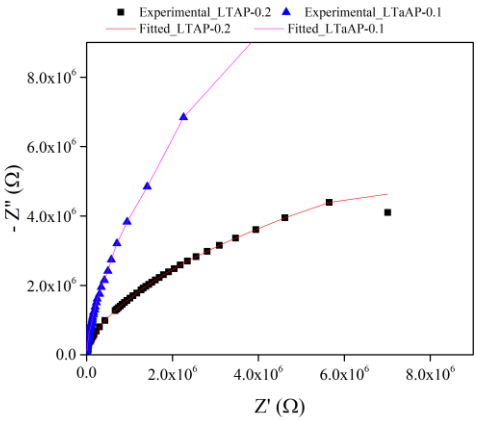

Fig. 5 Impedance spectra for LTAP-0.2 and LTaAP-0.1 composition

4 Conclusion

In this study, lithium titanium aluminium phosphate LTAP and lithium tantalum aluminium phosphate LTaAP NASICON-type solids electrolytes were successfully prepared using conventional solid-state technique. Optimum sintering parameter for LTAP and LTaAP compositions were successfully obtained at 800 °C sintering temperature. Bulk density of 2.92 and 3.52 g/cm^3 for LTAP and LTaAP were successfully obtained for the optimum sintering parameter which was an indication that both materials have been completely densified. XRD reveals prominent NASICON phases for LTAP compared to LTAaP composition. It is obvious that LTaAP crystalline peaks were dominated with $AlPO_4$ secondary phase which could hindered the movement of Li-ion conductivity, though some researchers reported that, for LTAP materials, $AlPO_4$ phase could act as sintering aid and improved material densification. Both compositions have the capacity to serve as solid electrolytes material that could be used in lithium ion rechargeable battery.

Acknowledgement

The authors are grateful to the Federal University of Technology Minna and University Tun Hussein Onn Malaysia (UTHM) for their support and funding; this work is funded under incentive for publication grant (IGSP), U412 and graduate research incentive grant (GIPS), U301, UTHM.

References

[1] N. Anantharamulu, K. Koteswara Rao, G. Rambabu, B. Vijaya Kumar, V. Radha, and M. Vithal, "A wide-ranging review on Nasicon type materials," *Journal of Materials Science*, vol. 46, no. 9, (2011) pp. 2821–2837.

[2] X. Xu, Z. Wen, Z. Gu, X. Xu, and Z. Lin, "Preparation and characterization of lithium ion-

conducting glass-ceramics in the $Li_{1+x}Cr_xGe_{2-x}(PO_4)_3$ system," *Electrochemistry Communications*, vol. 6, no. 12, (2004) pp. 1233–1237.

[3] M. Pérez-Estébanez, J. Isasi-Marín, D. M. Többens, A. Rivera-Calzada, and C. León, "A systematic study of Nasicon-type $Li_{1+x}M_xTi_{2-x}(PO_4)_3$ (M: Cr, Al, Fe) by neutron diffraction and impedance spectroscopy," *Solid State Ionics*, vol. 266, (2014) pp. 1–8.

[4] K. Arbi, R. Jimenez, T. Šalkus, A. F. Orliukas, and J. Sanz, "On the influence of the cation vacancy on lithium conductivity of $Li_{1+x}R_xTi_{2-X}(PO_4)_3$ Nasicon type materials," *Solid State Ionics*, vol. 271, (2015) pp. 28–33.

[5] K. Arbi, M. Ayadi-Trabelsi, and J. Sanz, "Li mobility in triclinic and rhombohedral phases of the Nasicon-type compound $LiZr_2(PO_4)_3$ as deduced from NMR spectroscopy," *Journal of Materials Chemistry*, vol. 12, no. Icmm, (2002) pp. 2985–2990.

[6] V. Thangadurai, A. K. Shukla, and J. Gopalakrishnan, "New lithium-ion conductors based on the NASICON structure †," *Journal of Materials Chemistry*, vol. 9, (1999) pp. 739–741.

[7] H. Morimoto, H. Awano, J. Terashima, Y. Shindo, S. Nakanishi, N. Ito, K. Ishikawa, and S. I. Tobishima, "Preparation of lithium ion conducting solid electrolyte of NASICON-type $Li_{1+x}Al_xTi_{2-x}(PO_4)_3$ (x = 0.3) obtained by using the mechanochemical method and its application as surface modification materials of LiCoO2 cathode for lithium cell," *Journal of Power Sources*, vol. 240, (2013) pp. 636–643.

[8] N. V. Kosova, E. T. Devyatkina, A. P. Stepanov, and A. L. Buzlukov, "Lithium conductivity and lithium diffusion in NASICON-type $Li_{1+x}Ti_{2-x}Al_x(PO_4)_3$ ($0 <= x <= 0.3$) prepared by mechanical activation," *Ionics*, vol. 14, no. 4, (2008) pp. 303–311.

[9] H. Rusdi, A. Abd Rahman, R. H. Y. Subban, and N. S. Mohamed, "Characterisation of Lithium Aluminium Titanium Phosphate as Solid Electrolytes Synthesized by Mechanical Milling Method," *Advanced Materials Research*, vol. 545, (2012) pp. 190–194.

[10] L. Xiong, Z. Ren, Y. Xu, S. Mao, P. Lei, and M. Sun, "LiF assisted synthesis of $LiTi_2(PO_4)_3$ solid electrolyte with enhanced ionic conductivity," *Solid State Ionics*, vol. 309, no. April, (2017) pp. 22–26.

[11] X. Lu, S. Wang, R. Xiao, S. Shi, H. Li, and L. Chen, "First-principles insight into the structural fundamental of super ionic conducting in NASICON $MTi_2(PO_4)_3$ (M = Li, Na) materials for rechargeable batteries," *Nano Energy*, vol. 2 (2017) pp 7 - 14.

[12] A. F. Orliukas, A. Dindune, Z. Kanepe, J. Ronis, B. Bagdonas, and A. Kežionis, "Synthesis and peculiarities of electric properties of $Li_{1.3}Zr_{1.4}Ti_{0.3}Al_{0.3}(PO_4)_3$ solid electrolyte ceramics," *Electrochimica Acta*, vol. 51, no. 27, (2006) pp. 6194–6198.

[13] S. Tamura, K. ichiro Araki, and N. Imanaka, "Trivalent gallium ion conduction in NASICON-type solid," *Journal of Asian Ceramic Societies*, vol. 4, no. 4, (2016) pp. 390–393.

[14] T. Salkus, A. Dindune, Z. Kanepe, J. Ronis, A. Urcinskas, A. Kezionis, and A. Orliukas, "Lithium ion conductors in the system $Li_{1+y}Ge_{2-x-y}Ti_xAl_y(PO_4)_3$ (x = 0.1÷0.3, y = 0.07÷0.21)," *Solid State Ionics*, vol. 178, no. 21–22, (2007) pp. 1282–1287.

[15] S. Wang, L. Ben, H. Lee, and L. Chen, "Identifying Li^+ ion transport properties of aluminium doped lithium titanium phosphate solid electrolytes at wide temperature range," *Solid State Ionics* vol 268, (2014) pp 110-116.

[16] Nda, M., Adnan, M. S., Ahmad, K. A., Usman, N., Razi, M. A. M., & Daud, Z. "A Review on the Causes, Effects and Mitigation of Climate Changes on the Environmental Aspects." *International Journal of Integrated Engineering*, vol. 10, no. 4 (2018) pp. 169 - 175.